Fault Detection and Diagnosis in Spacecraft Electrical Power Systems

Marc A. Carbone*
NASA Glenn Research Center, Cleveland, Ohio 44135
and
Kenneth A. Loparo†
Case Western Reserve University, Cleveland, Ohio 44106

https://doi.org/10.2514/1.I011136

The ability to accurately identify and isolate failures in the electrical power system (EPS) is critical to ensure the reliability of spacecraft. This paper proposes a novel solution to the problem of fault detection and diagnosis in direct current (DC) electric power systems for spacecraft. Autonomous operation becomes essential during deep space missions that lack the ability to monitor and control the spacecraft from ground locations. The current state of EPS fault supervision is insufficient to guarantee highly reliable operation. To solve this issue, a combination of model-based and knowledge-based techniques are used in a hierarchical framework to improve the diagnostic performance of the system. Noise, disturbances, and modeling errors are considered in the design of the fault detection system. Practical considerations related to spacecraft flight hardware and software are accounted for in the system design for flight applications. To assess the functionality of the design, a wide array of failures are simulated in a series of experiments. The experiments showed that the technique improved the capability of the autonomous system by increasing the number of fault types diagnosed. The significance of this study is to provide a framework capable of advanced diagnostics of an EPS with little to no interaction from human operators.

Nomenclature

F = set of possible faults, f, in a given system
$\boldsymbol{G}$ = input distribution matrix
$\boldsymbol{H}$ = output matrix
$\boldsymbol{K}$ = Kalman gain matrix
$\boldsymbol{P}$ = error covariance matrix
u = vector of control variables
v = vector of random measurement errors
w = vector of random variables
x = vector of state variables
$\boldsymbol{Y}$ = admittance matrix
z = vector of output variables (measurements)
$\boldsymbol{\Gamma}$ = noise distribution matrix
η = standardized innovation sequence
ν = innovation sequence
ρ = density
$\boldsymbol{\Phi}$ = state transition matrix

Subscript

k = discrete time step

I. Introduction

SPACE agencies around the world, including NASA, along with domestic and international partners, are working to solve the challenges of deep space exploration [1]. The increased distance between Earth-based mission control and the spacecraft will significantly increase communication delays and hamper ground-based communications and control. For example, communications from Earth to a Mars-based spacecraft are expected to take between 6 and 44 min round trip [2]. Further, even for crewed missions, the crew would not be able to carry out all of the necessary functions performed by mission control today due to the increasing complexity of the spacecraft. To solve these problems, higher levels of vehicle autonomy will be required to carry out the functions of deep space vehicles that have previously been done from the ground.

The electrical power system (EPS) of a spacecraft is one of the spacecraft systems that require improved automation to function in the deep space environment. The primary function of an electric power system is the reliable generation, transmission, and distribution of electric power to meet a randomly variable demand [3]. The same requirements are amplified for the electric power systems onboard spacecraft due to the increased risks associated with human space travel. A critical component of power system control is the ability to detect and diagnose faults quickly and accurately to serve critical loads and to prevent catastrophic blackouts on the spacecraft. Current efforts in fault detection and diagnosis (FDD) for spacecraft EPS relies on automatic protection and close monitoring from ground support personnel to diagnose any anomaly in the system. To make supervision a part of the autonomous control system several enhancements have to be made to the existing approaches. The current methods of supervision can be improved significantly by considering the information hidden in all measurements and automatic control actions that keep the system operational [4]. Current efforts in advanced direct current power system control include NASA's Gateway [5,6] and the lunar surface [7]. While DC microgrids present new opportunities for the future grid, the standards for control and management of DC microgrids require further development [8].

The core principle of power system operation is to maximize its reliability in meeting the load demand at minimum cost. The enabling technology to assure a high degree of reliability is fault detection, isolation, and recovery. A fault can be defined as an unintended deviation of at least one characteristic property or parameter of the system from the acceptable/usual/standard operating condition [9]. The process of fault supervision takes place in two steps. First, *fault detection* is defined as the binary decision to recognize that a fault occurred. Second, *fault diagnosis* is the task of finding the cause and location of the fault [4]. This paper addresses the FDD challenge within the context of DC microgrids on spacecraft. The goal of FDD is to achieve a quick and accurate diagnosis of the faulty components, facilitate decision making for corrective actions, and ensure timely responses to faults that can prevent component deterioration and

Received 12 April 2022; revision received 16 December 2022; accepted for publication 27 January 2023; published online 17 April 2023.

*Electrical Engineer, Power Management and Distribution; marc.a.carbone@nasa.gov.

†Arthur L. Parker Professor, Department of Electrical, Computer and Systems Engineering; kal4@case.edu.

performance degradation. The ability to make optimal reconfiguration decisions is largely dependent on the speed and accuracy of the detection and diagnosis. The task of fault diagnosis is made more challenging due to the wide variety of fault types that can lead to the degradation and failure of the power system. Faults in the sensors, actuators, communications, or controller can be obscured or amplified by closed-loop control, leading to inability to detect and diagnose the fault or damage to the system creating a dangerous environment for nearby humans. Therefore, there is a demand for more advanced supervisory functions responsible for identifying faults and taking action to maintain operation and avoid further damage [10].

Historically, research in FDD for aerospace EPS systems has utilized several approaches, including the Bayesian approach [11,12], the interacting multiple-model technique [13,14], optimization-based methods [15], the constraint suspension approach [16], and Kalman-filter-based methods [17]. More recent efforts in identifying faults in other aerospace subsystems include Ref. [18], which uses machine learning, a Kalman observer, and a decision tree to detect sensor failures; Ref. [19], which uses machine learning techniques to detect errors in aircraft actuation systems; and Ref. [20], which compares knowledge-based, model-based, and machine-learning-based approaches to identify multicopter rotor failures. Photovoltaic (PV) and power converter FDD is performed in Ref. [21] using an autoregressive modeling technique and in Ref. [22] using a model-based digital twin technique. Recursive least squares and an adaptive Kalman filtering (AKF) method are developed in [23] to detect series arc faults in DC distribution lines. DC arc faults are also diagnosed in [24], where an unknown input observer (UIO) method is used to diagnose the faulted line. System-level protection in DC microgrids for short-circuit faults and power electronic switches is achieved in [25] using a bank of H-infinity observers. Active-model-based fault diagnosis is applied to reconfigurable battery systems using the sigma point Kalman filter (SPKF) in [26]. Another Kalman-filter-based method is used to detect sensor faults in battery packs in [27]. This approach worked well for single faults of various types within a battery system consisting of battery cells, switches, and bus bars. In Ref. [28] a data-driven method using fuzzy Bayes risk and support vector machine is applied to the problem of satellite EPS fault diagnosis rather than model-based methods due to the unnecessary computational complexity of the current state-of-the-art. Interacting multiple-model estimation is applied to single and double faults in [29]. The current literature does not address some of the critical features needed for spacecraft EPS fault detection. The current gaps in the literature necessitate that enhanced methods should be capable of 1) diagnosing a wide array of fault types (including the components, sensors, and communication system), 2) diagnosing multiple faults in series, and 3) operating at realistic spacecraft telemetry update rates. These gaps serve as the motivation for this paper. Table 1 summarizes the performance characteristics of this paper with the previous works in the literature.

The unique contributions of this paper are as follows. First, the diagnostic engine can diagnose a wide range of fault types, including faults in the lines, switches, sensors, and communication system. The existing approaches are designed to support a very limited number of fault types, making them inflexible and limited in their applications in real-world scenarios. Rather than having several algorithms running to detect the wide array of possible faults, a single, comprehensive method is derived to distinguish between similar fault types. Second, the application is tailored for spacecraft EPS where only low telemetry update rates (1–10 Hz sampling frequency) are available. Many of the existing techniques rely on high-frequency data (>1 kHz). The proposed method addresses this issue through a hierarchical design that detects and isolates harmful faults quickly at the lower level of the controller, and diagnoses small and subtle faults at the higher level. Third, the proposed method provides the ability to adapt as the system evolves or degrades, especially in the context of cascading faults and failure events. This work demonstrates the ability to adapt the system model to continue monitoring for faults during 1) known changes to the system structure (e.g., changes in the distribution system topology), and 2) changes to the state of the system (e.g., existing faults in the system). Thus, allowing the controller to continue diagnosis after one or more faults have occurred. Fourth, due to the stringent computational requirements of spacecraft flight computers, supervisory algorithms have limited processing capability. In the classical multiple-model formulation for FDD, each fault model is tested in parallel when a fault is detected. The technique presented in this paper differs from other model-based approaches by reducing the number of parallel filters needed for testing using the lower-level algorithms. Information from the local devices provides information to the central controller, allowing it to limit the number of models passed through to the hypothesis testing function. This is accomplished through the unique integration of limit-checking and multiple-model-based techniques. The model generation, fault hypothesis, and decision-making functions developed in this paper are responsible for coordinating the two techniques and improving the overall diagnostic capability of the FDD system. The advantages of the technique proposed in this paper to the existing body of research for the application of spacecraft EPS are as follows:

1) The ability to detect and diagnose a wide variety of EPS faults, including sensors, actuators, communications, and power electronics
2) Dynamic model generation to adapt to changes in the system structure or parameters
3) The ability to detect and diagnose multiple faults in sequence
4) Reduction in computational complexity compared to existing model-based techniques

The proposed solution in this paper is based on the fundamental concept of hierarchical control that decomposes the control system functions into primary (local), secondary (supervisory), and tertiary (adaptive) layers. Local control requires the fastest time response as it is responsible for maintaining stability and dynamically managing disturbances, Supervisory control coordinates systemwide interactions to achieve optimal performance objectives, and adaptive control provides fault-tolerant behavior by modifying system control and performance objectives to respond to changes in operating conditions, such as those caused by faults and large disturbances. The proposed solution integrates knowledge-based systems with advanced multiple-model-based techniques in a way that increases the ability to detect and diagnose many fault types, while reducing overall computational complexity. The main features of this design are 1) direct layer algorithms that use

Table 1 Performance comparison of FDD approaches

Work	Application	Approach	Telemetry frequency	FDD of components	FDD of sensors	FDD of communication system	Maximum sequential faults diagnosed
[22]	PV systems	Digital Twin	500 kHz, 0.1 Hz	Yes	Yes	No	1
[23]	DC cables	RKF, AKF	100 kHz	Yes	No	No	1
[24]	DC cables	UIOs	200 kHz	Yes	No	No	1
[25]	DC microgrids	H-inf observers	1 MHz	Yes	No	No	1
[26]	Battery systems	Model based	25 Hz	Yes	Yes	No	1
[27]	Battery systems	Model based	— —	No	Yes	No	1
[28]	Satellite EPS	Data driven	cont.	Yes	No	No	1
[29]	F/A-18 aircraft	Multiple model	10 Hz	Yes	Yes	No	2
This work	Spacecraft EPS	Hybrid	1 Hz, 5 Hz	Yes	Yes	Yes	34

AKF, adaptive Kalman filtering; DC, direct current; EPS, electrical power system; FDD, fault detection and diagnosis; PV, photovoltaic ; RLS, recursive least squares; UIOs, unknown input observers.

local measurements to facilitate time requirements to isolate harmful faults, 2) supervisory layer algorithms that use systemwide data and contain the advanced diagnostic techniques that are needed to reliably diagnose low-magnitude faults of all types, and 3) an adaptive model generation approach that lowers the computational complexity needed at the supervisory level while maintaining diagnostic accuracy. Limitations on the spacecraft communications and computation equipment result in reduced measurement update rates to the controller. For example, the system proposed in this work relies on 5 Hz communications in the direct layer, and 1 Hz updates in the supervisory layer, which is typical of space flight communications hardware. Although this paper focuses on the application of FDD to space-based DC microgrids, the system can be adapted to a wide range of industrial applications that require high reliability, including terrestrial power systems, naval shipboard power systems, and autonomous vehicles. Machine learning techniques were not used in this work as they present new challenges related to validation and verification for flight-rated systems; however, they could be added to this framework as an area of future research.

The remainder of this paper is organized as follows: Section II formulates the problem of FDD. Section III outlines the algorithms and structure of the supervisory tool. Section IV discusses the strategy to diagnose faults in sequence. Lastly, Sec. V provides conclusions and remarks about the strengths and weaknesses of the approach.

II. Fault Detection and Diagnosis: Problem Formulation

The objective of FDD is to identify the (normal or faulted) state of an engineering system or process. More formally, fault or anomaly detection can be defined as a hypothesis testing problem [30], where the normal operation of the system is regarded as the null hypothesis. Data from the actual system are tested against the null hypothesis at a certain statistical significance threshold. The results of the tests can be used to determine the operational (normal or faulted) behavior of the system. After the occurrence of a fault is detected, the next step is then fault diagnosis. Together, these define FDD.

Consider a process with measurable input $u(t)$ and output $z(t)$ vectors. At any point of operation, a fault $f(t)$ can occur. Faults may occur due to a number of external factors, such as changes in environmental conditions (e.g., humidity, temperature, electromagnetic radiation), or internal causes like worn components, short circuits, leaks, and overheating, among others. The faults cause changes in the process

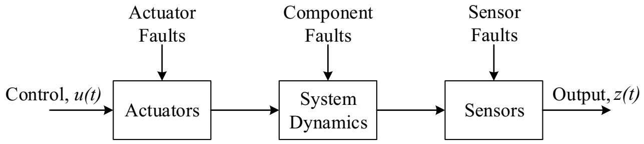

Fig. 1 Fault types based on process category: actuators, system dynamics, and sensors.

operating conditions that can be modeled as changes in parameters $\mathbf{\Phi}(t)$ by $\Delta\mathbf{\Phi}(t)$ and/or internal state variables $x(t)$ by $\Delta x(t)$. These changes lead to a change in the output $z(t)$ by $\Delta z(t)$. It can be increasingly difficult in closed-loop systems to detect and diagnose faults, as changes in the output $(\Delta z(t))$ can quickly be masked due to the feedback; however, permanent changes in $\Delta u(t)$ can be observed. System noise, disturbances, and modeling errors can corrupt $z(t)$, making FDD more challenging.

Due to the wide variety of potential fault types, more robust techniques are necessary to correctly diagnose and react to faults in a timely manner. A fault may be classified into one of the following three categories based on the way it has appeared in the system:

1) Abrupt (sudden) faults
2) Incipient (slowly developing) faults, i.e., drift faults
3) Intermittent faults

Abrupt faults appear when a significant change in a parameter or behavior has occurred rapidly. Often abrupt faults occur in systems where failures need to be detected early enough to prevent catastrophic damage or collapse of the entire system by fast corrective action. *Incipient* faults, however, are commonly associated with maintenance problems where early detection of worn equipment is required. In this situation faults are not catastrophic and typically difficult to detect, but the detection time is of less importance. Lastly, *intermittent* faults appear and disappear over time, making detection and diagnosis additionally challenging. A controlled process can be decomposed into three parts: actuators, system dynamics, and sensors (as shown in Fig. 1). Faults in these three parts of the system can occur, causing different behavior in the output or measurements $z(t)$. Examples of actuator faults include lock-in-place faults, hard-over faults, and float faults. Sensor faults can occur in many forms, such as bias faults, drift faults, hard-over faults, noise faults, stuck faults, calibration faults, and spike faults. Component faults are specific to the physics of the process, and therefore it is difficult to define common types. More details on fault type definitions can be found in [31].

III. Proposed FDD Methodology

The proposed hierarchical approach consists of two layers. The primary layer represents the device level of the EPS, where local data for components (i.e., switch-gear, power electronics, etc.) are collected and analyzed. In the primary layer, a bank of physics-based limit checks are used to quickly and accurately isolate harmful faults and faults easily detected by local data. The secondary layer of the controller resides at the global level of the controller, where telemetry from each of the spacecraft EPS components is collected. Here, a multiple-model dynamic state estimation approach is used to detect low-magnitude faults and sensor faults, and provide additional confirmation of faults detected at the device level based on the global behavior of the system. A block diagram of the hierarchical FDD method is shown in Fig. 2. The primary control FDD is used to help reduce complexity at the adaptive level of the system by providing

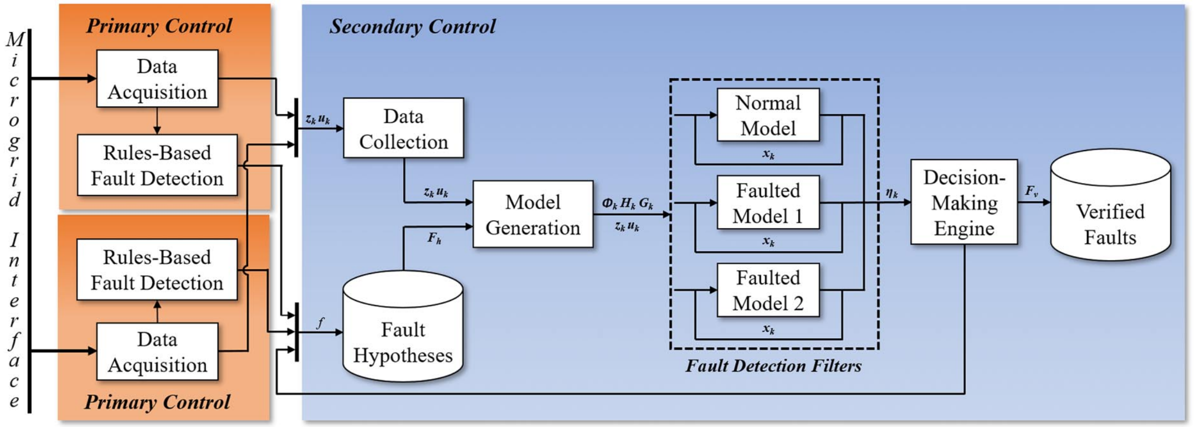

Fig. 2 Architecture of the hierarchical FDD method.

additional information to the fault hypothesis function responsible for generating the fault models. The novel feature of this method is the combination and coordination of the two methods within the hierarchy through the decision-making engine and fault hypothesis functions. This produces a diagnostic engine capable of detailed diagnostic performance using the multiple-model-based approach, while reducing the overall complexity of the implementation by using limit checking techniques in the direct layer. This practical solution is designed to solve the challenges related to spacecraft EPS fault diagnosis within the constraints of a spacecraft flight control architecture. The remainder of this section describes the decision-making process and objectives of the proposed control system.

A. Physics-Based Limit Checking

Knowledge-based rules for FDD are the most common techniques found in industry due to their simplicity and reliability [32]. Limit checking is a method often found in practice where measurements are compared to preset thresholds. Given a scalar measurement $z_i(t)$ from sensor i we can detect faults using the absolute value check

$$z_{i,\min} < z_i(t) < z_{i,\max} \tag{1}$$

where $z_{i,\min}$ and $z_{i,\max}$ are predetermined fault thresholds for sensor i. Figure 3 shows an example signal triggering upper and lower alarm thresholds. Many systems have two levels of alarms, one to indicate a warning and one for emergency reaction. A limit check can also be applied to the trend $\dot{z}_i(t)$ of the measurement $z_i(t)$ for sensor i. If the limit values are set appropriately, the fault alarm can take place earlier than the absolute value check because the trend provides an indication of the temporal progression of the signal.

As a general rule, limit checking methods should be based on the first principles physics of the system. This enables intuitive and reliable fault detection. Other methods of rule generation based on "expert knowledge" of the system can also be used but may cause conflict if the system structure changes. Traditionally, limit checking methods for monitoring and automatic protection are sufficient for the overall protection of the process; however, to set the correct tolerances for decision making, compromises must be made to obtain fast FDD. These methods may also trigger false alarms due to normal fluctuations in the variables, noise, or disturbances.

In this paper physics-based limit checking is used to simplify the computational power needed to diagnose faults. The direct layer of the control system receives measurements at the highest frequency. With high-resolution data, limit checking can be used to quickly detect faults where systemwide data are not required. This feature can relieve the computational burden of the supervisory layer, while supporting the time-critical actions needed in the direct layer.

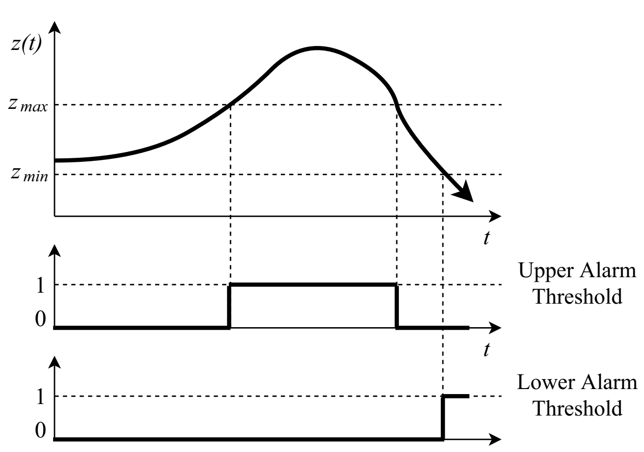

Fig. 3 Limit checking of signal $z(t)$.

B. Estimation-Based Method

Process models, estimators, and decision methods make it possible to estimate nonmeasurable variables such as process states and parameters, as well as predicting signals. This technique can be used to detect faults earlier and locate them more accurately than conventional limit and trend checks [33]. In model-based FDD a mathematical representation of the system is developed based on physical and statistical information. The model can be categorized in many ways, such as static or dynamic, linear or nonlinear, continuous or discrete, and deterministic or stochastic [34].

Most model-based FDD methods rely on analytical redundancy to determine the probability of faults [35,36] as shown in Fig. 4. Analytical redundancy is achieved using an explicit mathematical model as well as sensor measurements from the system. The appeal of analytical redundancy lies in the fact that additional information can be extracted from the existing information without adding physical equipment to the system. The difference between measured outputs $z(t)$ and the estimated model outputs $\hat{z}(t)$ define the estimation error otherwise known as residuals, which may be used to indicate that a fault has occurred in the system [37]:

$$e(t) = z(t) - \hat{z}(t) \tag{2}$$

Early approaches for FDD using mathematical models were developed in the mid-20th century (see [10,37–41] for a review). Among these methods are the fault detection filter [42], the innovation test using a single Kalman filter [34,43], banks of Kalman filters (or Luenberger observers) [44,45], the parity space method [46], and the parameter estimation approach [47].

The method in this paper relies on a multiple-model framework to diagnose low-magnitude faults and sensor faults. This technique is well suited for reconfigurable systems and also provides better diagnostic resolution by using several fault detection filters operating in parallel, each tailored to represent a particular event. The multiple-model approach is applied to sensor and actuator failures on the F-16 aircraft in [48]. Real-time monitoring and diagnostics for rotating machinery using a bank of stochastic nonlinear observers is developed in [49]. A nonlinear multiple-model filtering algorithm was used to detect leaks in a laboratory heat exchange process in [50]. This paper expands upon these works by considering a wider range of fault types and dynamically generating the system model, allowing it to adapt to changes in the system states and parameters.

1. Model Generation

Complex behavior of physical systems drives the need for effective models. Systems never truly operate in the steady state, and stochastic variations in the process can introduce significant uncertainties in the dynamic behavior of the state and output. The traditional techniques of steady-state estimation are often unable to accurately capture the dynamic behavior of the operational environment. Newer approaches, such as dynamic state estimation (DSE), are capable of accurately modeling and tracking changes in the system states over time [51].

To track the dynamic states of the system, the innovations-based framework proposed by [34] is used. The mathematical model developed for the process is based on physical and statistical data.

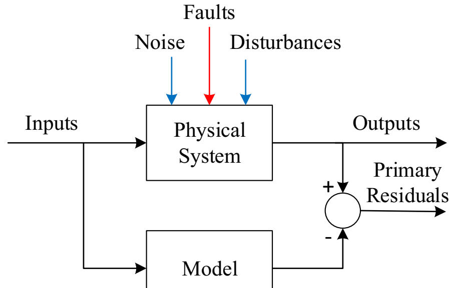

Fig. 4 Analytical redundancy of a physical system.

All inputs, outputs, and system parameters should be clearly defined. The nominal model should capture the behavior of the system under normal operation. To construct the model of the system, consider the discrete-time linear multi-input–multi-output (MIMO) process

$$x_{k+1} = \mathbf{\Phi} x_k + \boldsymbol{G} u_k + \mathbf{\Gamma} w_k \tag{3}$$

$$z_k = \boldsymbol{H} x_k + v_k \tag{4}$$

where x_k is an $n \times 1$ vector of state variables (subscript k indicates the time instant), u_k is a $p \times 1$ vector of control (input) variables, w_k is a $q \times 1$ vector of random variables, z_k is an $m \times 1$ vector of output variables (measurements or observations), $\mathbf{\Phi}$ is an $n \times n$ state transition matrix, $\boldsymbol{G}$ is an $n \times p$ input distribution matrix, and H is an $m \times n$ output matrix. $\mathbf{\Gamma}$ is an $n \times q$ noise distribution matrix, which modifies the $q \times 1$ vector of random variables w_k and adds to the state vector, and v_k is an $m \times 1$ vector of random measurement errors that add directly to the output measurements z_k. The random vectors w_k and v_k are assumed to be independent Gaussian white noise sequences with known mean and covariance matrices.

The Kalman filter is the best linear mean-square estimator of the state vector x_k given the input variables u_k and the measured output variables z_k. If it is assumed that all system parameters and statistics are known exactly, the innovation sequence of the Kalman filter can be generated in the following form:

$$\bar{x}_{k+1|k} = \mathbf{\Phi}[\bar{x}_{k|k-1} + \boldsymbol{K}_k \nu_k] + \boldsymbol{G}_k u_k + \mathbf{\Gamma}_k \bar{w}_k \tag{5}$$

$$\hat{x}_{0|-1} = x_0 \tag{6}$$

$$\nu_k = z_k - \boldsymbol{H}_k \hat{x}_{k|k-1} - \bar{v}_k \tag{7}$$

$$\boldsymbol{K}_k = \boldsymbol{P}_{k|k-1} \boldsymbol{H}_k^T (\boldsymbol{H}_k \boldsymbol{P}_{k|-1} \boldsymbol{H}_k^T + \boldsymbol{R}_k)^{-1} \tag{8}$$

$$\boldsymbol{P}_{k+1|k} = \mathbf{\Phi}_k \boldsymbol{P}_k \mathbf{\Phi}_k^T + \mathbf{\Gamma}_k \boldsymbol{Q}_k \mathbf{\Gamma}_k^T \tag{9}$$

$$\boldsymbol{P}_{k|k} = (\boldsymbol{I} - \boldsymbol{K}_k \boldsymbol{H}_k) \boldsymbol{P}_{k|k-1} \tag{10}$$

where $\boldsymbol{P}_{k|j}$ is the error covariance matrix of $\hat{x}_{k|j}$ such that $\boldsymbol{P}_{k|j} = E\{(x_k - \hat{x}_{k|j})(x_k - \hat{x}_{x|j})^T\}$, and $\boldsymbol{K}_k$ is the $n \times m$ Kalman gain matrix [52]. The innovation sequence ν_k is a vector representation of the difference between the system output measurements and model output estimates.

To support the dynamic generation of the system models, a *model generator* function receives real-time data about the system structure and hypothesized fault information to produce a model of the system under a particular operating condition. Information about a potential fault, including the type, location, and magnitude, can all be used to automatically populate the model. To determine which faults should be generated, a *fault hypothesis* function receives fault indications from the distributed limit-checking method and the output of the multiple-model-based method. More information about modeling faults can be found in [4,31]. The model generation function is critical in enabling highly adaptive FDD. This function creates a mapping between the EPS components and the mathematical model of the power system, so that changes in the power system (including faults) can be dynamically added into the model for fault testing. Multiple faults can be added into the model at once, for diagnosing a power system with multiple failures.

2. *Residual Signal Hypothesis Testing*

One of the reasons the Kalman filter is a convenient choice for FDD is that if the process and model parameter matrices match, then the statistics of the innovation sequence are well known; that is, the innovation sequence ν_k (which can be used as the residuals) is a zero mean Gaussian white noise sequence with covariance equal to

$$\operatorname{cov}(\nu_k) = \left(\boldsymbol{H}_k \boldsymbol{P}_{k|-1} \boldsymbol{H}_k^T + \boldsymbol{R}_k\right) \tag{11}$$

For fault isolation, it is more useful to consider the standardized innovation sequence

$$\eta_k = \left(\boldsymbol{H}_k \boldsymbol{P}_{k|-1} \boldsymbol{H}_k^T + \boldsymbol{R}_k\right)^{-1/2} \nu_k \tag{12}$$

where $(\cdot)^{-1/2}$ represents the square root of the inverse of a matrix so that

$$E\{\eta_k \eta_j^T\} = \boldsymbol{I} \delta_{k,j} \tag{13}$$

where I denotes the identity matrix and $\delta_{k,j}$ denotes the Kronecker delta.

The known statistics of the standardized innovation sequence simplifies the fault hypothesis testing for detecting faults such as sensor bias, noisy measurements, changes in the level of noise, and changes in the system parameters. These faults can be identified using the tests for whiteness, mean, and covariance described in [34].

C. Fault Hypothesis

In the classical multiple-model formulation each known fault model is tested in parallel when a fault is detected. This approach is burdensome for large systems with many measurements and fault types, where the controller must process the many additional computations required by each model added. This additional computation is impractical for spacecraft flight systems where processing resources are highly limited. This paper proposes a fault hypothesis function that is designed to determine the fewest number of faults that should be analyzed by a fault detection filter. This is achieved using information from the direct layer algorithms and the residuals of the normal model filter. To determine the set of fault detection filters, let F represent the set of possible faults $f_1, f_2, \ldots, f_n$ for a given system. Then define the set F_v to be the set of faults that have already been verified by the FDD method. The set F_h represents the set of fault hypotheses that are to be analyzed by the estimator. The objective of the FDD engine is to 1) use the bank of rules and innovations to determine which faults should be added to F_h, and 2) verify which fault(s) from F_h belong in F_v.

When a fault hypothesis f is generated by the direct or adaptive layers, an asynchronous message is sent to the fault hypothesis generator that determines which fault models should be generated and analyzed. The condition for a fault f_i to be added to the set F_h is

$$f_i \notin F_v \cup F_h \tag{14}$$

This straightforward but unique feature ensures that the detected fault has not already been diagnosed and added to the list of verified faults. It also checks that the fault is not already under analysis and has previously been added to the list of fault hypotheses. Using the collection of information of both knowledge-based and model-based methods, the fault hypothesis function can improve the completeness, resolution, and efficiency of the multiple-model approach.

D. Decision-Making Engine

The *decision-making engine* is a novel function added to the adaptive layer that is designed to take the results from the bank of fault models and decide if 1) a new fault has been detected, or 2) a fault hypothesis has been verified. The results of the normal model innovations are used to generate the new fault hypotheses. Tests of whiteness, mean, and covariance on the innovations are used to decide which fault type may have occurred [53]. For dynamic state estimators (filter systems) that do not produce white noise residuals, a whitening filter can be used to preprocess the data as shown in [54].

The first objective of the decision-making engine is to determine if any new fault hypotheses should be generated. System-specific faults, such as excessive vibration or anomalies in sensor data, may also cause changes in the mean or covariance. If tests for mean and covariance fail, a new fault hypothesis is generated that corresponds to the results of the statistical tests. In addition, a bank of known faults based on a known direction of the innovation vector, η, are analyzed in the event of a fault detection. If $\hat{\eta}$ (the conditional mean of η) points in the direction of one of the known faults, a new fault hypothesis is generated and added to the set of fault hypotheses, F_h. Faults detected at this level may require system-wide data that are not available at the direct layer, such as sensor faults or subtle current leaks in distribution lines. This unique feature of the FDD method helps reduce the number of fault models that need to be analyzed and increases the accuracy of the method through the statistical analysis of the innovations.

The second responsibility of the decision-making engine is to validate the current state of the system, that is, to determine which faults (if any) have been validated by the FDD method. To do this, tests on the mean and covariance of the innovations are applied to each of the fault detection filters. The fault filter that passes all of the statistical tests is determined to correspond to a valid fault and is added to the set of verified faults F_v. Similarly, if faults are removed from the system, the corresponding system model should be analyzed and tested to validate the updated fault state of the system.

A challenge in this approach is developing models that capture the unique dynamic behaviors of the system and the qualities of each fault type to reduce the risk of having multiple fault detection filters simultaneously pass the innovations tests. Careful considerations should be taken into account for the design of the fault models to increase isolability. For many systems, certain faults may appear indistinguishable depending on available sensor (measurement) data. In cases where more than one model passes all of the statistical tests, a number of actions may be taken. If human operators have direct access to the system, the remaining fault hypotheses can be sent for further manual diagnostics. Alternatively, autonomous systems can use a bank of rules to prioritize certain faults based on operator experience, historical/reliability data, or fault severity, or by using an active fault diagnostic approach [55] to probe the system to generate additional data that can be used to separate the overlapping fault hypotheses.

IV. Application to Spacecraft DC Microgrid

In this section, the proposed FDD solution is applied to a spacecraft power system. The DC electrical system in this study is made up of interconnected PV arrays controlled by maximum power point tracking, batteries regulated by DC/DC converters under droop control, distribution lines and bus bars, and a combination of resistive, constant power, and alternating current (AC) motor (M) loads. The design goals for this system are to detect and diagnose a wide range of faults, including line-to-ground faults, distribution switch failures, and sensor and communication system malfunctions. The level of criticality of these faults varies; however, each fault type poses a risk to the overall performance and reliability of the microgrid. Therefore, it is important for the diagnostic engine to identify each fault type so that proper corrective actions can be taken. The FDD design for each control layer is described below.

A. Direct Level

For the spacecraft application, limit-checking methods and automatic protection are deployed at the direct control level, and switch failures in the distribution system can easily be detected at this level. This fault type differs from short-circuit protection, where a low-impedance path to ground causes a current inrush and a relay to trip. Instead, a failed switch occurs when the observed state (open or closed) does not match the physical state of the switch. For example, a distribution switch may become fused shut and may not respond to commands to open it. This can lead to power outages and power flow imbalances. Algorithm 1 is used to detect the failed switches using physics-based limit checking. Measurements V_{IN}, V_{OUT}, I_{IN}, and I_{OUT} refer to the input voltage, output voltage, input current, and output current of each distribution switch, respectively. The *state* variable refers to the binary status of the switch (open or closed).

Here, $\Delta V_{\max}$ represents the maximum tolerable potential difference for a closed switch, and $I_{\max}$ represents the maximum tolerable current that can be observed through an open switch. Both values are predefined by the system operator and must be set to tolerate the noise in the measurements.

Algorithm 1: Switch failed open/closed

for each switch **do**
  $\Delta V = |V_{IN} - V_{OUT}|$
  $I_{avg} = \frac{1}{2}(I_{IN} + I_{OUT})$
  if $\Delta V > \Delta V_{max}$ **and** $state = closed$ **then**
    FaultDetected(*SwitchFailedOpen*)
  end if
  if $I_{avg} > I_{max}$ **and** $state = open$ **then**
    FaultDetected(*SwitchFailedClosed*)
  end if
end for

Algorithm2: Fault detected

if $faultType_n \in faultMap$ **then**
  $r = NumRepititions(faultType_n)$
  if $r < maxRepititions$ **then**
    $r = r + 1$
  else
    if $r = maxRepititions$ **then**
      PublishFaultToSecondaryControl($faultType_n$)
    end if
  end if
else
  $faultMap \rightarrow$ AddFault($faultType_n$)
end if

For highly critical faults that could interrupt EPS operation, such as line-to-ground faults, circuit breakers and relays are used to measure the current and voltage of a particular location and isolate the fault. In the case of a short to ground, a *di/dt*-based technique can be used to detect the fault quickly and reliably. The critical nature of these faults requires them to use high-frequency measurements at the device level. Once the fault is detected, the fault information (location, type, size, etc.) is captured in the device-level controller and sent to the central controller so that further analysis and reconfiguration can be performed.

To reduce the number of false alarms generated by the knowledge-based system, a voting scheme is used to track the number of consecutive times a fault is detected as shown in Algorithm 2. Any fault status is checked to see if the fault has been observed r consecutive times before passing the fault message to the supervisory controller. This reduces the occurrence of false fault alarms caused by noise, disturbances, and modeling errors.

B. Adaptive Level

At the adaptive level of the control system, a linear time-invariant (LTI) model of the spacecraft power system is generated using the electrical topology of the distribution network. Modifying the solution for the AC power flow in [56] produces the nodal DC power flow equations that are used to generate the admittance matrix $\boldsymbol{Y}$ of the distribution system as follows:

1) Diagonal elements $\boldsymbol{Y}_{ii}$ = sum of admittances connected to bus *i*.

2) Off-diagonal elements $\boldsymbol{Y}_{in} = -$ (sum of admittances connected between bus *i* and *n*) for $i \neq n$.

Then the nodal equations for the distribution system are

$$I = \boldsymbol{Y}V \tag{15}$$

where I is the vector of currents injected into each bus, and V is the vector of bus voltages. For bus i the corresponding nodal equation is

$$I_i = \sum_{n=1}^{N} \boldsymbol{Y}_{in} V_j \tag{16}$$

The real power at any bus i is

$$P_i = V_i I_i \tag{17}$$

These equations are used to generate the output matrix $\boldsymbol{H}$ that relates the measurements to the state variables. The state of each distribution switch, S_i, is monitored such that

$$S_i = \begin{cases} 1 & \text{if switch } i \text{ reads closed} \\ 0 & \text{if switch } i \text{ reads open} \end{cases} \tag{18}$$

The admittance model can dynamically adapt to changes in the distribution system by including the measured switch states into the model such that

$$I_i = \sum_{n=1}^{N} S_i S_n \boldsymbol{Y}_{in} V_n \tag{19}$$

thus allowing the power flow model to represent both connected and disconnected lines in the model.

Let the state vector x_k be defined as the vector of bus voltages in the power system, $x^T = [V_1, V_2, \ldots V_n]$. Measurement vector z_k is the set of current and voltage measurements in the distribution system at time k. To make this model of the distribution system applicable to any DC microgrid, no model of the controller is required. Therefore, the input vector u_k and the matrix $\boldsymbol{G}_k$ are not used in the model. The state update matrix $\boldsymbol{\Phi}_k$ is equal to an identity matrix. $\boldsymbol{R}_k$ is a diagonal matrix of the sensor variances. $\boldsymbol{Q}_k$ a matrix of zeros when the innovations pass the statistical tests. When the innovations fail one or more of the tests, the process covariance $\boldsymbol{Q}_k$ is an identity matrix. The dynamic process covariance is used to filter out disturbances caused by the Markovian jump states of the power system that model the occurrences of faults in the system and also provides optimal data smoothing in the steady state.

V. Computer Simulation and Results

To verify the performance of the solution, a series of fault tests are conducted using a simulation of a 120 V DC spacecraft electric power system developed in Mathworks' MATLAB/Simulink. A one-line diagram of the system architecture is shown in Fig. 5. The simulation is generated based on a library of Thevenin equivalent power system component models and provides accurate, high-frequency characteristics of the electric power system. Inputs to the simulation include distribution switch states, battery charge/discharge unit (BCDU) droop parameters, solar array, and energy storage parameters. The key power system parameters are given in Table 2. The distribution line parameters used to generate the FDD admittance matrix are shown in Table 3. The simulation output consists of the line currents, node voltages, distribution switch states, and the status of circuit breakers. To emulate spacecraft telemetry, communications data are sent to the local device controllers at 5 Hz, and the supervisory level control receives data at 1 Hz. Note that 171 current and voltage measurements are available to the controller to perform analysis. The data are synchronized using a polling technique from an open-source C++ messaging software. The data from the experiments are captured from the C++ controller code and visualized using the MATLAB.

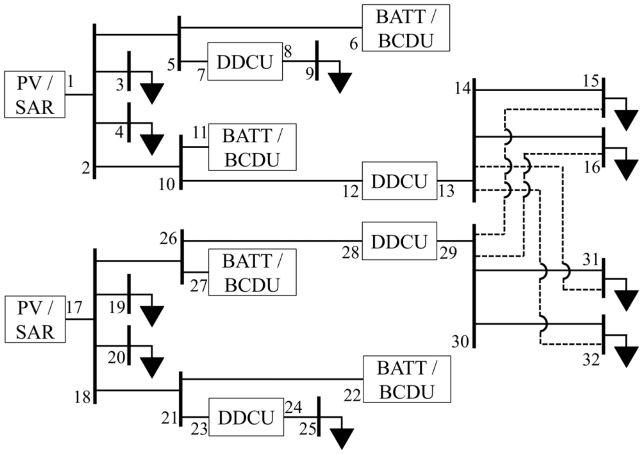

Fig. 5 One-line diagram of the test spacecraft power system.

Table 2 Spacecraft EPS parameters

Description	Value
Nominal SAR output voltage	123 V
Nominal BCDU voltage set point	120 V
Battery charging droop slope	100 V/A
Battery discharge droop slope during	21.25 V/A
Battery capacity	176.6 A · h
Nominal DDCU voltage set point	122.8 V
Load per PDU	0.96 kW
Measurement update rate of the device controllers	5 Hz
Measurement update rate of the central controller	1 Hz
Standard deviation of voltage measurement error	0.24
Standard deviation of current measurement error	0.12

BCDU, battery charge/discharge unit; DDCU, DC/DC converter unit; PDU, power distribution unit; SAR, solar array regulator.

Table 3 Distribution line parameters

From bus	To bus	R (Ω)
1	2	0.005
2	3	0.105
2	4	0.105
2	5	0.025
2	10	0.03
5	6	0.005
5	7	0.105
8	9	0.097
10	11	0.025
10	12	0.105
13	14	0.104
14	15	0.005
14	16	0.005
14	31	0.005
14	32	0.005
17	18	0.005
18	19	0.105
18	20	0.105
18	21	0.025
18	26	0.03
21	22	0.005
21	23	0.105
24	25	0.097
26	27	0.025
26	28	0.105
29	30	0.104
30	15	0.005
30	16	0.005
30	31	0.005
30	32	0.005

It is important to note that the models used in the EPS simulation are not used in the development of the mathematical model for the FDD system. This way, as there will be in any physical application, there is a mismatch between the actual microgrid process (simulation) and the models used to develop the FDD system. Treating these models as separate entities helps improve the usefulness of the simulation testing because it treats the power system behavior with some unknowns and uncertainty, similar to that of a hardware test bed.

The voltage and current measurements from the computer simulation under normal operation are shown in Fig. 6, where measurements (blue) and estimates from the DSE (red) are shown before and after a disturbance caused by a change in load. The sample rate of the data provided in the figures is at the 1 Hz supervisory control rate. Notice that near the time of the disturbance, the process covariance

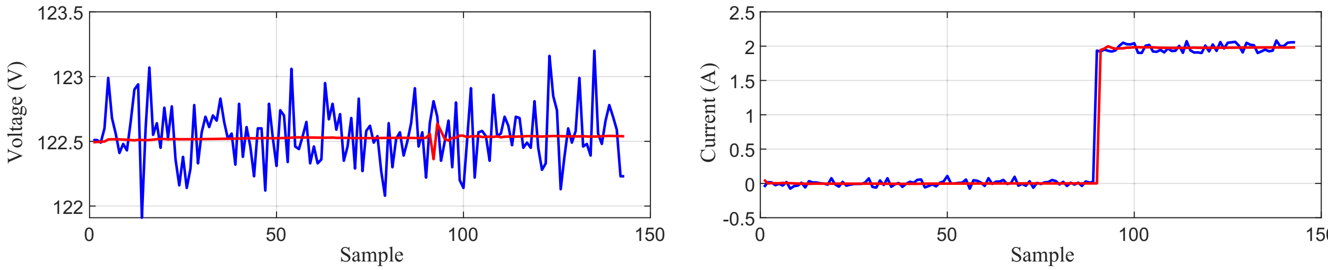

Fig. 6 Simulation data (blue) and Kalman estimates (red) during change in load.

adapts to provide rapid convergence. For this application, the innovation sample window N is set equal to 5 (samples) to provide quick FDD.

The simulation supports over 385 unique fault types that are capable of being inserted and removed from the power system at any time. First, a test of each fault was conducted, where each fault was inserted individually. The results confirmed that the FDD method successfully identified each of the 385 faults. The following subsections will demonstrate the behavior and response of the FDD system for a few of these faults.

A. Distribution Switch Failure

The first fault type under consideration is a failed distribution switch. In this case, a switch has failed open when commanded to be closed at sample 317. This causes the current between nodes to drop to zero, as seen in Fig. 7c. Note that the state estimator attempts to track the disturbance; however, the discrepancies in the node voltages provided by the model Figs. 7a and 7b fail the test of zero mean while the fault is detected and diagnosed in samples 317 through 324.

The limit checking algorithm triggers a failed switch fault message via Algorithm 1. The adaptive control layer generates a fault model based on the current measurements and sets the corresponding stuck switch to open due to the fault message. This model is then processed and is successful in passing all of the statistical tests. Once the tests have passed, the fault is published and the switch fault model is redefined as the updated operational model of the power system. At sample 328 the fault is repaired, and the system returns to the normal state.

B. Incipient Sensor Offset

The previous case was an example of an abrupt fault. Next, we examine the case of an incipient fault in the form of a sensor offset. In this situation the sensor bias will increase slowly over time. These faults are challenging to detect, as the impact of the fault on the measurement will initially be small, and difficult to detect in the presence of noise. However, it is important to detect such faults quickly, so that impacts to other processes such as voltage regulation will be minimized. Figure 8a shows the results of a node voltage sensor during an incipient sensor fault. Measurements are displayed in blue, and the estimate is in red. The fault is inserted at sample 50, the fault is diagnosed, and the measurement is removed from the DSE at sample 86 because the measurement is no longer valid. The fault is recovered at sample time 96, where the FDD service recognizes that the sensor has returned to normal operation and adds the measurement back into the model at sample 101.

Figure 8b displays the innovations of the signal in black against the threshold for the test of zero mean in red. The fault is detected at sample 80 when the mean of the residual crosses the threshold. A fault model for the sensor fault is generated and passes all of the innovations tests. At sample 86 the fault model residuals pass the tests, and the fault is detected and diagnosed.

C. Communication Failure

A communication failure is one category of fault that may occur in any system that uses a communication network for data transfer and control. These faults are dependent on the physical attributes of the network as well as the software implementation of the communication system. For this experiment, a communication fault is generated where messages are blocked from a direct layer device to the supervisory layer. A polling system is used to collect data from each of the direct layer systems when a data request message is sent by the supervisory controller. If the supervisory controller has not received updated data from the direct layer, it will send its last set of data cached in memory. On each iteration of the data acquisition process,

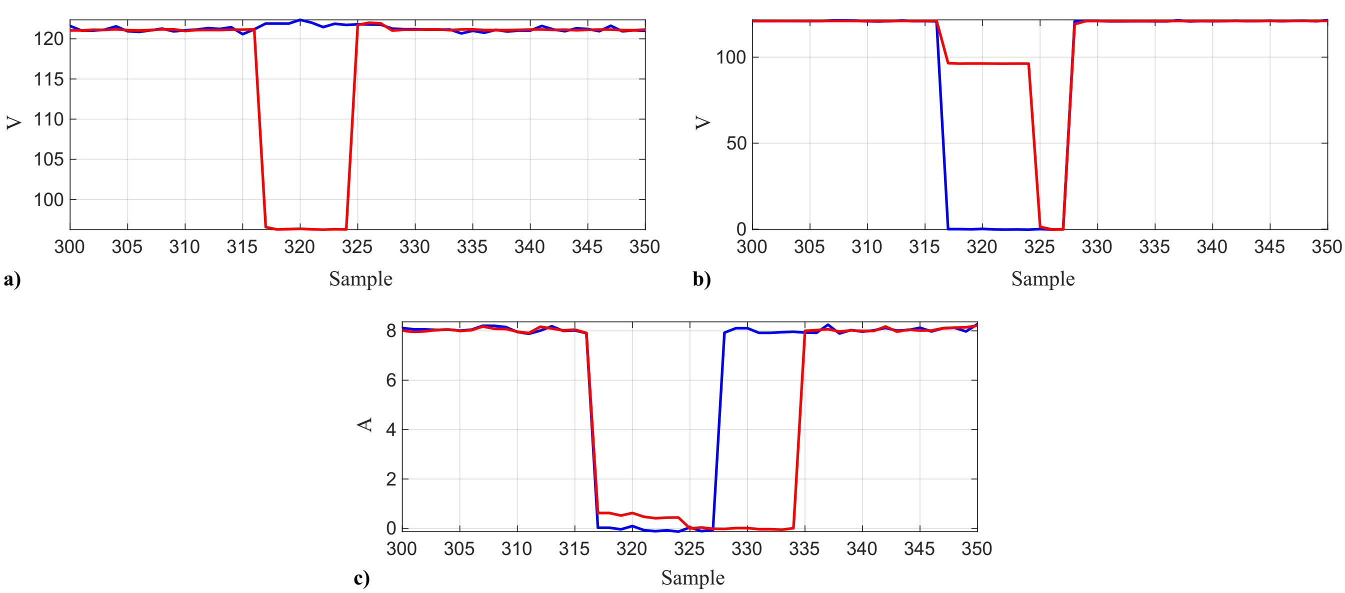

Fig. 7 Measurements (blue) and estimates (red) during the FDD response to a failed distribution switch: a) distribution switch input voltage, b) distribution switch output voltage, and c) distribution switch current.

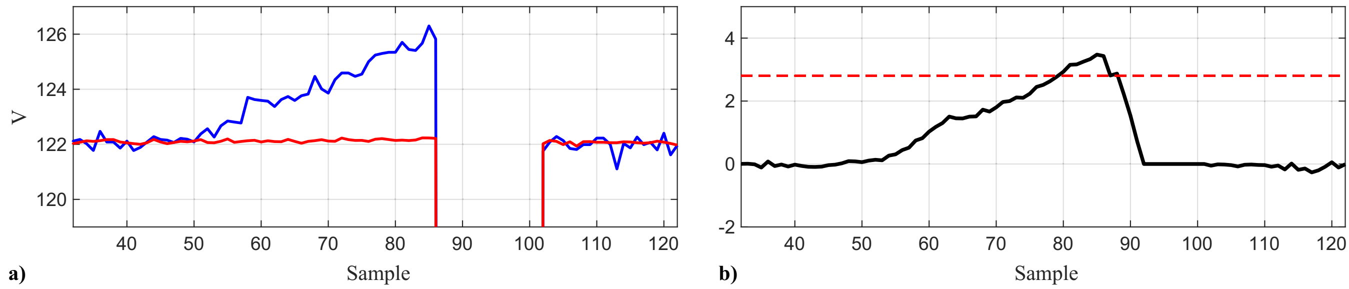

Fig. 8 a) Measurement (blue) and estimate (red) of the faulty voltage sensor. b) Innovations of the faulty sensor.

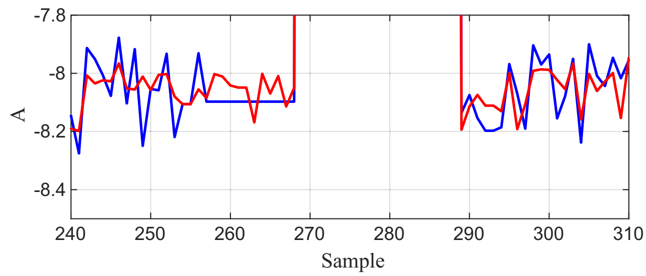

Fig. 9 Dynamic state estimation during a communication failure.

the supervisory layer controller checks the range of timestamps for stale data. If one or more data packets exceed the maximum timestamp lag, a stale data fault is generated.

Figure 9 shows measurements and data before, during, and after the communication fault. A model is generated for this fault by eliminating the corresponding rows in the output matrix. A test for observably is used to ensure that the DSE can be performed with the missing data. To validate the faulty behavior, the test for whiteness must fail for the measurements. Once the fault is removed and data begin to publish as normal, the nonfaulted model passes the statistical tests, thus validating the removal of the communication fault as seen from samples 290 through 310. The benefit of this approach is that estimates for the missing data are still generated during the communication failure, which provides necessary information to the controller while the device is unable to communicate.

D. Multiple Fault Diagnosis

The ability to troubleshoot failures, repair equipment, or perform component maintenance for many systems is often limited due to the availability of onsite maintenance crews. Therefore, it is critical to have an adaptive diagnostic system that is capable of fault monitoring even after there are changes (e.g., faults) to the system. For example, if a faulty sensor is detected in the network, the FDD method should be capable of reconciling the faulty data through state estimation, then continue monitoring for additional faults that may occur before the sensor fault can be resolved. Further, if a distribution switch fails and is stuck open, the controller should reconfigure the network as needed and continue monitoring the system. This process should occur until the power system is fully degraded or there are insufficient data to identify further faults. The limited ability to repair or replace components in the space environment indicates the need for more adaptable fault detection and diagnostic control methods.

To measure the adaptive capabilities of the proposed method, several experiments are conducted where faults are injected into the DC microgrid system simulation in sequence until the FDD engine is no longer able to correctly diagnose the fault. Because the number of possible fault combinations grows exponentially with time, a Markov chain (MC) model is used to randomly generate faults in the power system. One hundred randomly generated fault sequences are used to determine the accuracy and performance of the FDD method. During each sequence, a fault is randomly generated from the MC and inserted into the simulation. If the fault is correctly diagnosed within a set period of time, the automated test system records the results, and a new fault is generated. If the fault is not detected or diagnosed correctly, the incorrect result is recorded, and the test sequence ends. Upon failure, all the faults are cleared from the simulation and the method is reset to the normal condition, and the next test sequence begins.

The results of the 100 MC tests are shown in Table 4. The performance of the FDD engine can be characterized by the mean number of faults that are detected and correctly diagnosed. In this study, an average of 11 faults were diagnosed by the system in each test. Figure 10 shows the number of faults correctly diagnosed in series for each test. Depending on the combination of faults selected at random, the number of identified faults ranged from 2 to 34. Insufficient data from sensor and communication faults are the main cause of failure to diagnose sequential faults. Furthermore, degradation caused by multiple hard faults, such as line-to-ground faults, can lead to missed detection or incorrect diagnosis as failures are masked by the blackouts within the power system. Overall, the FDD method proved to be successful in adapting to the changes in the system.

The proposed novel method improves upon the state-of-the-art by increasing the diagnostic capability of the controller in the presence of existing faults. Systems with extremely high reliability requirements such as deep space exploration stand to benefit from this work as the enhanced diagnostic performance will increase the overall system reliability.

Table 4 Markov chain experiment test results

Parameter	Value
Number of tests	100
Total number of faults inserted	1200
Mean faults diagnosed	11
Standard deviation	6.75
Minimum sequential faults diagnosed	2
Maximum sequential faults diagnosed	34

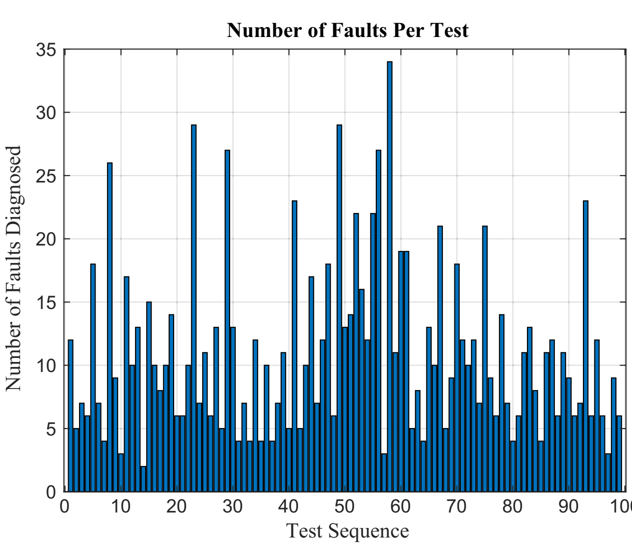

Fig. 10 Number of faults successfully diagnosed in each sequential fault test.

VI. Conclusions

In this paper, a novel method for FDD for a spacecraft EPS is developed. The decision-making principles used in this technique are hierarchical and structured as follows. Rules-based limit checking provided quick detection for critical failures that can be detected locally. This information is passed on to the central layer controller, reducing the overall complexity by limiting the set of fault hypotheses necessary to diagnose a fault. Also, the rules bank assisted in the integration of heritage FDD schemes, which often rely heavily on limit checking alarms. The multiple-model method in the central layer detects low-magnitude faults and sensor faults using the concept of analytical redundancy and provides the basis for isolating fault modes that may appear similar. The decision-making engine and fault hypothesis methods determine the minimum set of fault models needed for hypothesis testing. This solution can identify a wide range of fault types, including faulted sensors, actuators, cables, communication links, and power electronics. The fault models are generated dynamically; thus faults can be diagnosed even after changes in the system have occurred. This feature improves overall system autonomy and furthers the state-of-the-art in spacecraft EPS diagnostics. More robust FDD such as this can also benefit the controller by providing greater detail about the magnitude, location, and type of faults that may exist in the system.

Future work in this area may include integrating other methods of FDD such as machine learning techniques into the reactive and component layer controllers. Classifiers such as convolutional neural networks can be used to identify faults from high-resolution data based on known features of the transient signals. This capability could help improve the coordination between transient and steady-state FDD at the direct and adaptive layers. Further integration of FDD methods may provide more robust diagnostic capabilities, leading to more reliable system operation.

Acknowledgments

This work was funded by NASA's Exploration Systems Development Mission Directorate/Exploration Capabilities. The authors would like to thank NASA's Exploration Systems Development Mission Directorate/Exploration Capabilities for funding this work and the Advanced Modular Power Systems team, including Karin Bozak, Jim Soeder, Jeffrey Csank, Matthew Muscatello, Jeffrey Follo, Matthew Granger, and Brian Tomko, for supporting this work.

References

[1] Aaseng, G., Frank, J., Iatauro, M., Knight, C., Levinson, R., Ossenfort, J., Scott, M., Sweet, A., Csank, J., Soeder, J., Ngo, T., and Greenwood, Z., "Development and Testing of a Vehicle Management System for Autonomous Spacecraft Habitat Operations," *AIAA Space Forum*, AIAA Paper 2018-5148, 2018.
https://doi.org/10.2514/6.2018-5148

[2] Frank, J., Spirkovska, L., McCann, R., Wang, L., Pohlkamp, K., and Morin, L., "Autonomous Mission Operations," *2013 IEEE AerospacCe Conference*, Inst. of Electrical and Electronics Engineers, New York, 2013, pp. 1–20.
https://doi.org/10.1109/AERO.2013.6496927

[3] Loparo, K., and Abdel-Malek, F., "A Probabilistic Approach to Dynamic Power System Security," *IEEE Transactions on Circuits and Systems*, Vol. 37, No. 6, 1990, pp. 787–798.
https://doi.org/10.1109/31.55036

[4] Isermann, R., *Fault-Diagnosis Systems: An Introduction from Fault Detection to Fault Tolerance*, Springer Science & Business Media, Berlin, 2006.

[5] Csank, J. T., Soeder, J. F., Carbone, M. A., Granger, M. G., Tomko, B. J., Muscatello, M. J., and Follo, J. C., "A Control Framework for Autonomous Smart Grids for Space Power Applications," *International Astronautical Congress (IAC)*, NASA Technical Report Server, Washington, D.C., 2019, pp. 1–6.

[6] Carbone, M., Sajadi, A., and Loparo, K., "Bifurcation Analysis of DC Electric Power Systems for Deep Space Exploration Spacecraft," *2019 IEEE Power and Energy Conference at Illinois (PECI)*, Inst. of Electrical and Electronics Engineers, New York, 2019, pp. 1–7.
https://doi.org/10.1109/PECI.2019.8698916

[7] Csank, J., and Soeder, J., "Microgrid for Lunar Surface Power," *Lunar Surface Innovation Consortium–Lunar Surface Power Focus Group March Tag-Up*, NASA Technical Report Server, Washington, D.C., 2021, pp. 1–14.

[8] Patterson, B. T., "DC, Come Home: Dc Microgrids and the Birth of the "Enernet"," *IEEE Power and Energy Magazine*, Vol. 10, No. 6, 2012, pp. 60–69.
https://doi.org/10.1109/MPE.2012.2212610

[9] Hwang, I., Kim, S., Kim, Y., and Seah, C. E., "A Survey of Fault Detection, Isolation, and Reconfiguration Methods," *IEEE Transactions on Control Systems Technology*, Vol. 18, No. 3, 2010, pp. 636–653.
https://doi.org/10.1109/TCST.2009.2026285

[10] Frank, P. M., "Fault Diagnosis in Dynamic Systems Using Analytical and Knowledge-Based Redundancy: A Survey and Some New Results," *Automatica*, Vol. 26, No. 3, 1990, pp. 459–474.
https://doi.org/10.1016/0005-1098(90)90018-D

[11] Ricks, B. W., and Mengshoel, O. J., "Methods for Probabilistic Fault Diagnosis: An Electrical Power System Case Study," *Annual Conference of the PHM Society*, Vol. 1, PHM Society, 2009, pp. 1–20.

[12] Mengshoel, O. J., Darwiche, A., Cascio, K., Chavira, M., Poll, S., and Uckun, N. S., "Diagnosing Faults in Electrical Power Systems of Spacecraft and Aircraft," *AAAI*, nasa.gov, 2008, pp. 1699–1705.

[13] Zhang, L., and Li, X. R., "Detection and Diagnosis of Sensor and Actuator Failures Using IMM Estimator," *IEEE Transactions on Aerospace and Electrical Systems*, Vol. 34, No. 4, 1998, pp. 1293–1313.
https://doi.org/10.1109/7.722715

[14] Keller, K., Swearingen, K., Sheahan, J., Bailey, M., Dunsdon, J., Przytula, K. W., and Jordan, B., "Aircraft Electrical Power Systems Prognostics and Health Management," *2006 IEEE Aerospace Conference*, Inst. of Electrical and Electronics Engineers, New York, 2006, pp. 1–12.
https://doi.org/10.1109/AERO.2006.1656087

[15] Gorinevsky, D., Boyd, S., and Poll, S., "Estimation of Faults in DC Electrical Power System," *2009 American Control Conference*, Inst. of Electrical and Electronics Engineers, New York, 2009, pp. 4334–4339.
https://doi.org/10.1109/ACC.2009.5160301

[16] Fesq, L., and Ksenia, K., "Model-Based Off-Nominal State Isolation and Detection System for Autonomous Fault Management," *2016 IEEE Aerospace Conference*, Inst. of Electrical and Electronics Engineers, New York, 2016, p. 1.

[17] Nag, P. S., Kumar Silla, G., Gummadi, V. H. V., Harishankar, C., Ray, V. K., and Kumar, C. S., "Model Based Fault Diagnosis of Low Earth Orbiting (LEO) Satellite Using Spherical Unscented Kalman Filter," *IFAC-PapersOnLine*, Vol. 49, No. 1, 2016, pp. 635–638.
https://doi.org/10.1016/j.ifacol.2016.03.127

[18] de Silva, B. M., Callaham, J., Jonker, J., Goebel, N., Klemisch, J., McDonald, D., Hicks, N., Nathan Kutz, J., Brunton, S. L., and Aravkin, A. Y., "Hybrid Learning Approach to Sensor Fault Detection with Flight Test Data," *AIAA Journal*, Vol. 59, No. 9, 2021, pp. 3490–3503.
https://doi.org/10.2514/1.J059943

[19] Berri, P. C. C., Dalla Vedova, M. D. L., and Mainini, L., "Real-Time Fault Detection and Prognostics for Aircraft Actuation Systems," *AIAA Scitech 2019 Forum*, AIAA Paper 2019-2210, 2019.
https://doi.org/10.2514/6.2019-2210

[20] Dutta, A., McKay, M. E., Kopsaftopoulos, F., and Gandhi, F., "Multicopter Fault Detection and Identification via Data-Driven Statistical Learning Methods," *AIAA Journal*, Vol. 60, No. 1, 2022, pp. 160–175.
https://doi.org/10.2514/1.J060353

[21] Chen, L., Li, S., and Wang, X., "Quickest Fault Detection in Photovoltaic Systems," *IEEE Transactions on Smart Grid*, Vol. 9, No. 3, 2016, pp. 1835–1847.
https://doi.org/10.1109/TSG.2016.2601082

[22] Jain, P., Poon, J., Singh, J. P., Spanos, C., Sanders, S. R., and Panda, S. K., "A Digital Twin Approach for Fault Diagnosis in Distributed Photovoltaic Systems," *IEEE Transactions on Power Electronics*, Vol. 35, No. 1, 2019, pp. 940–956.
https://doi.org/10.1109/TPEL.2019.2911594

[23] Gajula, K., Marepalli, L. K., Yao, X., and Herrera, L., "Recursive Least Squares and Adaptive Kalman Filter Based State and Parameter Estimation for Series Arc Fault Detection on DC Microgrids," *IEEE Journal of Emerging and Selected Topics in Power Electronics*, Vol. 10, No. 4, 2021, pp. 4715–4724.
https://doi.org/10.1109/JESTPE.2021.3135409

[24] Yao, X., Le, V., and Lee, I., "Unknown Input Observer-Based Series DC Arc Fault Detection in DC Microgrids," *IEEE Transactions on Power Electronics*, Vol. 37, No. 4, 2021, pp. 4708–4718.
https://doi.org/10.1109/TPEL.2021.3128642

[25] Wang, T., Liang, L., Gurumurthy, S. K., Ponci, F., Monti, A., Yang, Z., and De Doncker, R. W., "Model-Based Fault Detection and Isolation in DC Microgrids Using Optimal Observers," *IEEE Journal of Emerging and Selected Topics in Power Electronics*, Vol. 9, No. 5, 2020, pp. 5613–5630. https://doi.org/10.1109/JESTPE.2020.3045418

[26] Schmid, M., Gebauer, E., Hanzl, C., and Endisch, C., "Active Model-Based Fault Diagnosis in Reconfigurable Battery Systems," *IEEE Transactions on Power Electronics*, Vol. 36, No. 3, 2020, pp. 2584–2597. https://doi.org/10.1109/TPEL.2020.3012964

[27] Xiong, R., Yu, Q., Shen, W., Lin, C., and Sun, F., "A Sensor Fault Diagnosis Method for a Lithium-Ion Battery Pack in Electric Vehicles," *IEEE Transactions on Power Electronics*, Vol. 34, No. 10, 2019, pp. 9709–9718. https://doi.org/10.1109/TPEL.2019.2893622

[28] Suo, M., Zhu, B., An, R., Sun, H., Xu, S., and Yu, Z., "Data-Driven Fault Diagnosis of Satellite Power System Using Fuzzy Bayes RISK and SVM," *Aerospace Science and Technology*, Vol. 84, Jan. 2019, pp. 1092–1105. https://doi.org/10.1016/j.ast.2018.11.049

[29] Zhang, Y., and Li, X. R., "Detection and Diagnosis of Sensor and Actuator Failures Using IMM Estimator," *IEEE Transactions on Aerospace and Electronic Systems*, Vol. 34, No. 4, 1998, pp. 1293–1313. https://doi.org/10.1109/7.722715

[30] Stuart, A., and Kendall, M. G., *The Advanced Theory of Statistics*, Griffin, London, 1963.

[31] Huang, S., Tan, K. K., Er, P. V., and Lee, T. H., *Intelligent Fault Diagnosis and Accommodation Control*, CRC Press, Boca Raton, FL, 2020, Chap. 2. https://doi.org/10.1201/9780429263880

[32] Gertler, J., *Fault Detection and Diagnosis*, Wiley Online Library, 2013.

[33] Gertler, J., *Fault Detection and Diagnosis in Engineering Systems*, Vol. 1, Marcel Dekker, New York, 1998, Chap. 1-2. https://doi.org/10.1201/9780203756126

[34] Mehra, R. K., and Peschon, J., "An Innovations Approach to Fault Detection and Diagnosis in Dynamic Systems," *Automatica*, Vol. 4, No. 5, 1971, pp. 637–640. https://doi.org/10.1016/0005-1098(71)90028-8

[35] Rauch, H. E., "Intelligent Fault Diagnosis and Control Reconfiguration," *IEEE Control Systems*, Vol. 14, No. 3, 1994, pp. 6–12. https://doi.org/10.1109/37.291462

[36] Chow, E., and Willsky, A., "Analytical Redundancy and the Design of Robust Failure Detection Systems," *IEEE Transactions on Automatic Control*, Vol. 29, No. 7, 1984, pp. 603–614. https://doi.org/10.1109/TAC.1984.1103593

[37] Willsky, A. S., "A Survey of Design Methods for Failure Detection in Dynamic Systems," *Automatica*, Vol. 12, No. 6, 1976, pp. 601–611. https://doi.org/10.1016/0005-1098(76)90041-8

[38] Himmelblau, D. M., *Fault Detection and Diagnosis in Chemical and Petrochemical Processes*, Vol. 8, Elsevier Science, 1978.

[39] Isermann, R., "Process Fault Detection Based on Modeling and Estimation Methods—A Survey," *Automatica*, Vol. 20, No. 4, 1984, pp. 387–404. https://doi.org/10.1016/0005-1098(84)90098-0

[40] Isermann, R., "Fault Diagnosis of Machines via Parameter Estimation and Knowledge Processing—Tutorial Paper," *Automatica*, Vol. 29, No. 4, 1993, pp. 815–835. https://doi.org/10.1016/0005-1098(93)90088-B

[41] Gertler, J. J., "Survey of Model-Based Failure Detection and Isolation in Complex Plants," *IEEE Control Systems Magazine*, Vol. 8, No. 6, 1988, pp. 3–11. https://doi.org/10.1109/37.9163

[42] Beard, R. V., "Failure Accomodation in Linear Systems Through Self-Reorganization," Ph.D. Thesis, Massachusetts Inst. of Technology, Cambridge, MA, 1971.

[43] Willsky, A., and Jones, H., "A Generalized Likelihood Ratio Approach to the Detection and Estimation of Jumps in Linear Systems," *IEEE Transactions on Automatic Control*, Vol. 21, No. 1, 1976, pp. 108–112. https://doi.org/10.1109/TAC.1976.1101146

[44] Clark, R. N., Fosth, D. C., and Walton, V. M., "Detecting Instrument Malfunctions in Control Systems," *IEEE Transactions on Aerospace and Electronic Systems*, Vol. 1, No. 4, 1975, pp. 465–473. https://doi.org/10.1109/TAES.1975.308108

[45] Montgomery, R., and Caglayan, A., "A Self-Reorganizing Digital Flight Control System for Aircraft," *12th Aerospace Sciences Meeting*, AIAA Paper 1974-0021, 1974.

[46] Deckert, J., Desai, M., Deyst, J., and Willsky, A., "F-8 DFBW Sensor Failure Identification Using Analytic Redundancy," *IEEE Transactions on Automatic Control*, Vol. 22, No. 5, 1977, pp. 795–803. https://doi.org/10.1109/TAC.1977.1101598

[47] Kitamura, M., "Detection of Sensor Failures in Nuclear Plants Using Analytic Redundancy," Oak Ridge National Lab., CONF 800607-46, TN, 1980.

[48] Menke, T. E., and Maybeck, P. S., "Sensor/Actuator Failure Detection in the Vista F-16 by Multiple Model Adaptive Estimation," *IEEE Transactions on Aerospace and Electronic Systems*, Vol. 31, No. 4, 1995, pp. 1218–1229. https://doi.org/10.1109/7.464346

[49] Loparo, K. A., Adams, M. L., Lin, W., Abdel-Magied, M. F., and Afshari, N., "Fault Detection and Diagnosis of Rotating Machinery," *IEEE Transactions on Industrial Electronics*, Vol. 47, No. 5, 2000, pp. 1005–1014. https://doi.org/10.1109/41.873208

[50] Loparo, K. A., Buchner, M., and Vasudeva, K. S., "Leak Detection in an Experimental Heat Exchanger Process: A Multiple Model Approach," *IEEE Transactions on Automatic Control*, Vol. 36, No. 2, 1991, pp. 167–177. https://doi.org/10.1109/9.67292

[51] Zhao, J., Gómez-Expósito, A., Netto, M., Mili, L., Abur, A., Terzija, V., Kamwa, I., Pal, B., Singh, A. K., Qi, J., and Huang, Z., "Power System Dynamic State Estimation: Motivations, Definitions, Methodologies, and Future Work," *IEEE Transactions on Power Systems*, Vol. 34, No. 4, 2019, pp. 3188–3198. https://doi.org/10.1109/TPWRS.2019.2894769

[52] Kalman, R. E., and Bucy, R. S., "New Results in Linear Filtering and Prediction Theory," *Journal of Basic Engineering*, Vol. 83, No. 1, 1961, pp. 95–108. https://doi.org/10.1115/1.3658902

[53] Mehra, R. K., "On the Identification of Variances and Adaptive Kalman Filtering," *IEEE Transactions on Automatic Control*, Vol. AC-15, No. 2, 1970, pp. 175–184. https://doi.org/10.1109/TAC.1970.1099422

[54] Carbone, M. A., "Development of a Supervisory Tool for Fault Detection and Diagnosis of DC Electric Power Systems with the Application of Deep Space Vehicles," Ph.D. Thesis, Case Western Reserve Univ., Cleveland, OH, 2021, http://rave.ohiolink.edu/etdc/view?acc_num=case1601984256665471.

[55] Punčochář, I., and Škach, J., "A Survey of Active Fault Diagnosis Methods," *IFAC-PapersOnLine*, Vol. 51, No. 24, 2018, pp. 1091–1098. https://doi.org/10.1016/j.ifacol.2018.09.726

[56] Glover, J., Sarma, M., and Overbye, T. J., *Power Sytem Analysis and Design*, Cengage Learning, Stamford, CT, 2012, pp. 978–981.

D. Casbeer
Associate Editor